The Synthesis of MnFe$_2$O$_4$-Activated Carbon Composite for Removal of Methyl Red From Aqueous Solution

Fahma Riyanti, Poedji Loekitowati Hariani[*,] Widia Purwaningrum, Elfita, Shella Santika, Iqlima Amelia

Department of Chemistry, Faculty of Mathematics and Natural Science, Sriwijaya University, Palembang, Indonesia

[*]email: puji_lukitowati@mipa.unsri.ac.id

ABSTRACT

In this study, MnFe$_2$O$_4$-activated carbon composite was synthesized by co-precipitation method and applied to adsorb methyl red dye. MnFe$_2$O$_4$-activated carbon composite was made with the mass ratio of activated carbon and MnFe$_2$O$_4$ of 1:2. The composite characterization by using X-Ray Diffraction, Fourier Transform Infrared Spectroscopy, Scanning Electron Micrograph, and Energy-Dispersive X-Ray Spectroscopy, the surface area using the Brunauer, Emmett and Teller and magnetic properties by using Vibrating Sample Magnetometer. The adsorption parameters include contact time, and adsorbent weight. The spectra of FTIR MnFe$_2$O$_4$-activated carbon composite analysis show the presence of Fe-O and Mn-O which is not present in the spectra of activated carbon. SEM analysis shows that the composite has pores and MnFe$_2$O$_4$ oxides are spread on its surface. The composition of the composite consists of C, O, Fe, and Mn. The composite has a surface area of 143.992 smaller than that of the activated carbon of 217.697 m^2/g. However, the composite has magnetic properties with the saturatization magnetization of 17.91 emu/g. The optimum condition of the composite for adsorption of methyl red was obtained at a weight of 0.15 g, and contact time of 100 minutes. The adsorption of the composite was in accordance by pseudo-second-order kinetic and Langmuir isotherms with adsorption capacity of 81.97 mg/g.

Keywords: Activated carbon, MnFe$_2$O$_4$, composite, adsorption, methyl red

INTRODUCTION

Activated carbon is an adsorbent that is often used in waste treatment. The adsorption process by using activated carbon has an advantage because the active carbon has a large porosity and surface area. Also, the adsorption process occurs rapidly, and it can be used to adsorb various compounds with a simple and regenerable design (Tan, Ahmad, & Hameed, 2008; Djilani et al., 2015). To increase the adsorption capacity, the activated carbon can be combined with other materials so that it has new properties as we desire.

Magnetic ferrite nanoparticle is a material of concern to be developed in recent years because it has unique magnetic and electrical properties. This material has different properties in its bulk (Deraz, & Alarifi, 2012; Aslibeiki et al., 2016). Magnetic ferrite has many uses. In the field of physics, it functions as magnetic sensors, broadband transformer, ferrofluids, etc. In the biomedical field, it functions as drug delivery, biosensor, magnetic resonance imaging, etc. and it has some functions also in the environmental field. One of the magnetic ferrites is MnFe$_2$O$_4$. The magnetic suspension of MnFe$_2$O$_4$ is higher than of the other ferrites such as MgFe$_2$O$_4$, CoFe$_2$O$_4$, ZnFe$_2$O$_4$ and NiFe$_2$O$_4$ with the magnetic spin of 5μb (Zhong, Yang, Chen, Qiu, & Zhang, 2015; Tawainella et al., 2014). Also, MnFe$_2$O$_4$ is superior mechanical and luminescent (Kanagesan et al., 2016).

The use of MnFe$_2$O$_4$ as an adsorbent has the advantage of a nano-size material so that it has a large surface area. After the adsorption process, the adsorbent can be pulled easily and quickly from the solution by using magnets because MnFe$_2$O$_4$ has magnetic properties. Several studies have used MnFe$_2$O$_4$ for the adsorption of both organic and inorganic pollutants, for example to removal of Pb (II) and Cu (II) (Ren et al., 2012), congo red (Zhong et al., 2015), phosphate (Xia et al., 2016), chromium (Sezgin, Yalcin, & Koseoglu, 2016), and rhodamin B (Riyanti, Hariani, & Purwaningrum, 2018).

Various methods can be used to synthesize MnFe$_2$O$_4$ such as mechanochemical reaction (Osmokrovic, Jovalelic, Manojlovic, & Pavlovic, 2006), sol-gel (Li, Yuan, Liu, & Leng, 2010; Shanmugavel, Raj, Kumar, & Rajarajan, 2014), hydrothermal (Hou, Feng, Xu, & Zhang, 2010), soft chemical route (Sam,

& Nesaraj, 2011), solid combustion route (Deraz, & Alarifi, 2012), microwave combustion (Sezgin et al., 2016), solvothermal (Aslibeiki et al., 2016), co-precipitation (Riyanti et al., 2018). The co-precipitation method is often used because it is simple, and the material obtained is more homogeneous (Audi, 2017). Riyanti et al. (2018) reported that $MnFe_2O_4$ synthesized using $MnCl_2$ and $FeCl_3$ precursors had a high saturation magnetization of 48.9 emu/g.

In this study, a composite synthesis from activated carbon and $MnFe_2O_4$ was done by using the co-precipitation method. The formation of nanomagnetic composites can increase the adsorption capacity and the efficiency of the adsorption process. The $MnFe_2O_4$-activated carbon composite produced was used to adsorb methyl red dyes. Yamaguchi, Bergamasco, & Hamoudi (2016) reported that the synthesized $MnFe_2O_4$-graphene composite using a one-pot facile method has a larger adsorption capacity than that of $MnFe_2O_4$ and graphene.

The methyl red is an anionic dye having a molecular formula $C_{15}H_{15}N_3O_2$ with a molecular weight of 269.30 g/mol (Khan, Shahjahan, & Khan, 2018). Methyl red has an azo group (-N = N-). This dye is widely used in industry in the coloring process because it has a bright and stable color. Synthetic dye is reported to cause carcinogenesis, respiratory toxicity, mutagenic in living organisms, skin irritation, chromosomal fractures, and teratogenicity (Santhi, Manonmani, & Smitha, 2010; Saxena, & Sharma, 2016). The presence of dyes in waters with low concentrations (<1 mg/L) may prevent sunlight from entering the waters, thus interfering with the process of photosynthetic plankton (Khan et al., 2018). Therefore, the treatment of wastewater containing synthetic dyes is very necessary before it is discharged into the environment.

EXPERIMENTAL SECTION

Chemical

The activated carbon used in this study is a local product having a surface area of 217.697 m^2/g, moisture content and ash content of 14.179 and 6.518%. The high purity chemicals include $MnCl_2.4H_2O$, $FeCl_2.4H_2O$, NaOH, KOH, and HCl of Merck. Methyl Red of Sigma Aldrich with cash number of 493-52-7. The equipment used consisted of standard laboratory glassware, UV-Vis Spectroscopy (Genesys 20), XRD Rigaku Miniflex 600, FTIR (Shimadzu 5000), SAA Quantrachrome Nova Win, SEM-EDS (6510 LA), VSM Oxford Type 1.2T.

Synthesis of Activated Carbon $MnFe_2O_4$-Activated Carbon Composite

The synthesis of $MnFe_2O_4$-activated carbon composite was done by dissolving 3.958 g of $MnCl_2.4H_2O$ and 10.812 g $FeCl_3.4H_2O$ g in 25 mL of distilled water at room temperature, 4.613 g $MnFe_2O_4$ was stoichiometrically formed. This calculation is based on the following reaction:

$2MnCl_2 + 4FeCl_3 + 16NaOH \rightarrow 2MnFe_2O_4 + 16NaCl + 8H_2O$
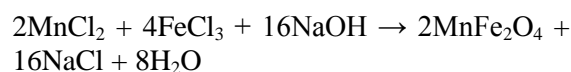
Into this mixture, 2.307 g of activated carbon was added. This mixture was stirred, and NaOH 5 M was slowly added until its pH reached $\pm$ 10. The stirring was continued for 30 minutes. The composite is separated from the solution using a magnet. Then washed with distilled water until neutral pH and heated in the oven at 100 °C for 2 hours. The composites were then determined by pHpzc and characterized by using FTIR, SEM-EDS, and SAA.

Determination of pH Point Zero Charge

A total of 50 mL of a 0.01M $NaNO_3$ solution was put respectively into 11 Erlenmeyer. The initial pH of the solution was adjusted from 2-12 by adding 0.1M HCl or 0.1M NaOH solution. Then into each Erlenmeyer, 0.2 g of the composite was added, it was shaken by a shaker for 2 hours. The mixture was allowed to stand for two days and measured its final pH using pH meters of each solution.

Adsorption Process

The adsorption process was carried out by the batch method. An amount of 100 mL of 100 mg/L methyl red solution (pH 4.4) was placed in a glass bottle, 0.15 g of $MnFe_2O_4$-activated carbon composite was added. The experiment was performed at room temperature. The glass bottle was placed on the shaker, stirring was done in the range of 10-140 minutes with a speed of 150 rpm. The adsorbent was separated from the solution using a permanent magnet. The concentration of the remaining dye was measured using a UV-Vis spectrophotometer at λ 490 nm. The effect of adsorbent weight was measured by

0.05-0.3 g adsorbent weight variation, whereas adsorption isotherm was measured using concentration of methyl red from 50-100 mg/L, the adsorbent weight of 0.15 g and contact time of 100 minutes.

RESULTS AND DISCUSSION

Characterization of MnFe₂O₄-activated carbon composite

Figure 1 displays the XRD pattern of $MnFe_2O_4$ and $MnFe_2O_4$-activated carbon composite. The composite peak is wide than $MnFe_2O_4$. Besides that, the peak on the composite has a lower intensity. It is influenced by the presence of amorphous activated carbon on the composite. $MnFe_2O_4$ ferrite phase is appear at 2θ = 29.94, 35.02, 43.22, 56.34 and 64.42°. The peak associated with the hkl value of (220), (311), (400), (511) and (440) (JCPDS no. 74-2403).

The analysis with FTIR was performed on activated carbon and $MnFe_2O_4$-activated carbon composite. Both spectra have a major

difference in the wave number of 515.0 cm^{-1} indicating the presence of manganese ferrites vibrations which were not found in the activated carbon spectra. Hidarian, & Hishemian (2014) reported the characteristics of the presence of $MnFe_2O_4$ on the composite appearing at wave numbers of 415-691 cm^{-1}. The similar result reported Riyanti et al. (2018) obtained at wave number 561.10 cm^{-1} as the vibration of Mn-O. The FTIR spectra of the $MnFe_2O_4$-activated carbon composite and the activated carbon are shown in **Figure 2.**

The comparison of the wave number of activated carbon and $MnFe_2O_4$-activated carbon composite is shown in **Table 1**. The wave number of 3382.9 cm^{-1} in the composite shows the presence of stretching and bending O-H groups. The peak that appears at the wave number of 2920.0 cm^{-1} shows the vibration of C-H. The wave number at 1562.2 cm^{-1} shows the presence of the C=C group. The presence of C-O was identified at wave numbers 1267.1 cm^{-1}.
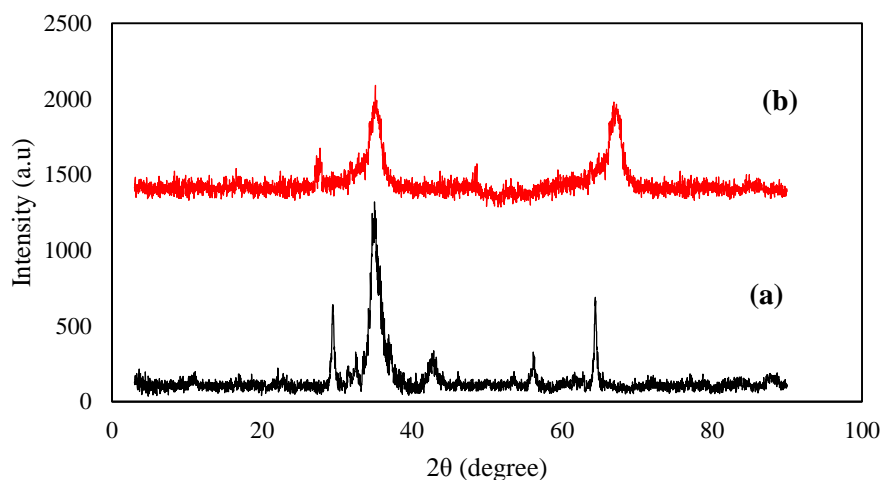
Figure 1. X-ray diffraction of (a) MnFe₂O₄ and (b) MnFe₂O₄-activated carbon composite
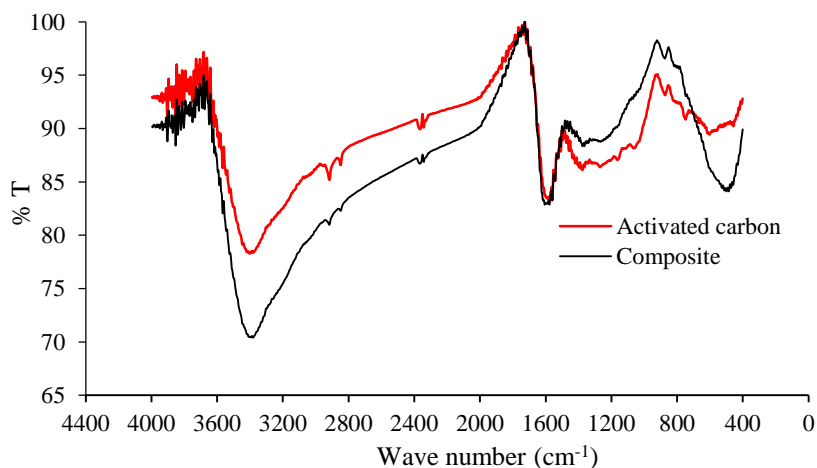
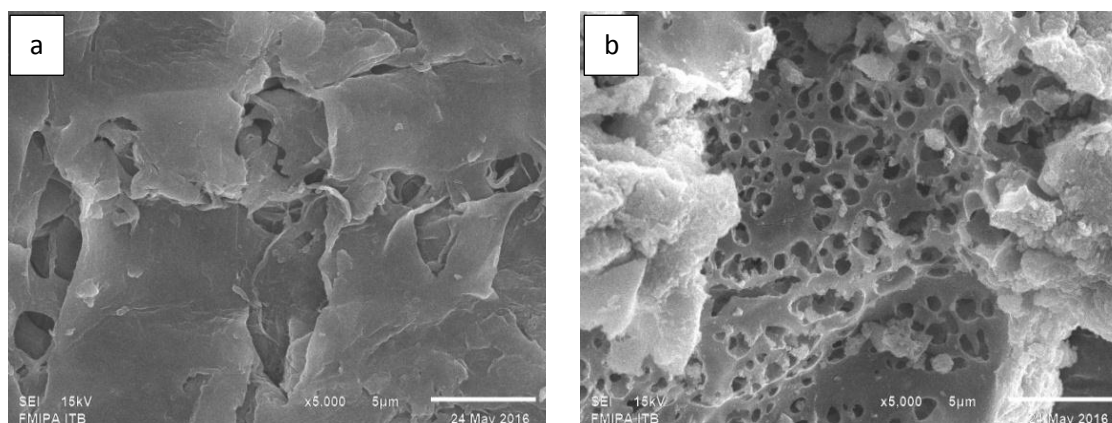**Figure 2.** FTIR spectra of activated carbon and MnFe₂O₄-activated carbon composite

The morphology of the activated carbon and MnFe$_2$O$_4$-activated carbon composite identified using SEM with 5000 x magnification is shown in **Figure 3**. In the Figure, it can be observed that the activated carbon has a surface morphology with wide, nonhomogeneous porous. The MnFe$_2$O$_4$-activated carbon composite has more pores and tends to be uniform with smaller pore sizes than those of the activated carbon. This occurs because of the addition of MnFe$_2$O$_4$ on the activated carbon which causes the oxide to enter the pores and is also dispersed randomly on the composite surface. **Table 2** shows the results of EDS analysis.

Activated carbon contains a major element of carbon at 98.92 %, and oxygen in a small percentage of 1.08 %. The addition of MnFe$_2$O$_4$ to the activated carbon causes a decrease in carbon content and an increase of O, Fe, and Mn. This proves that the composite synthesis process has been successful. The presence of Cl on the composite shows that there is still the remain of Cl from the synthesis process that has not been lost during the washing process. This is also reinforced by the data of the measurement of surface area in which the activated carbon used has a surface area of 217.697 m^2/g, with the addition of MnFe$_2$O$_4$ the surface area decreases to 143.992 m^2/g. However, with the addition of MnFe$_2$O$_4$, the activated carbon may have magnetic properties. The result of the measurement of magnetic properties using VSM is shown in **Figure 4**.

Table 1. The Comparison of the wave number of activated carbon and MnFe$_2$O$_4$-activated carbon composite

Functional groups	Wave number (cm^{-1})	Activated carbon (cm^{-1})	Composite (cm^{-1})
O-H	3200-3600	3404.1	3382.9
C-H	2850-2970	2918.1	2920.0
C=C	1500-1680	1562.2	1562.2
C-O	1050-1300	1164.9	1267.1
Fe-O, Mn-O	453-580	-	515.0

Figure 3. SEM micrograph of (a) Activated carbon (b) MnFe$_2$O$_4$-activated carbon composite

Table 2. The Elements of activated carbon and MnFe$_2$O$_4$-activated carbon composite

| Elements	Percentage of Mass (%)	
	Activated carbon	MnFe$_2$O$_4$-activated carbon composite
C	98.92	76.65
O	1.08	5.16
Cl	-	0.72
Mn	-	6.94
Fe	-	10.95

The activated carbon composite-MnFe$_2$O$_4$ has a magnetization saturation of 17.91 emu/g. The value of the saturation magnetization of the composite is smaller than that of the MnFe$_2$O$_4$. Riyanti et al. (2018) synthesize MnFe$_2$O$_4$ using co-precipitation methods to obtain a saturation magnetization of 48.90 emu/g. The study by Do et al. (2011) showed that the greater the nano ferrites content in the composite so the stronger the magnetic properties and the smaller the surface area. The active carbon pore space is blocked by nano-sized magnetic ferrites. The magnetic properties of this composite have the advantage, the separation of adsorbents from the solution can be done quickly using magnets without filtering, more effective and economical than non-magnetic adsorbents.

pH pzc (point zero charges) is a state in which the positive and the negative charges on the surface of a substance are equal so that the surface is neutrally charged. **Figure 5** shows the pH pzc of the MnFe$_2$O$_4$-activated carbon composite and activated carbon. The composite has a pH pzc of 5 indicating that at that pH the composite surface is neutral. At pH <5 the composite group is positively charged so that it attractive the anion more easily, whereas at pH > 5 the composite surface is negatively charged so that it is easier to adsorb the cation. The activated carbon has a pH pzc 6 that is bigger than composite.

Adsorption Study

The adsorption process of methyl red using activated carbon and MnFe$_2$O$_4$-activated carbon composite was performed at pH of methyl red solution of ± 4.4. Methyl red dye is an anionic dye having a pH range of 4.2-6.2. In that pH range, the dye is negatively charged, while the adsorbent is positively charged (pH solution <pH pzc), so that the tensile pull between the dye and the adsorbent is more effective. Other studies have reported that the methyl red adsorption process is effective at pH 4 using activated carbon from Annona squmosa seed (Santhi et al., 2010) and activated carbon from coconut husk (Tan et al., 2008).

Figure 6 shows the effect of contact time on methyl red adsorption process using activated carbon and MnFe$_2$O$_4$-activated carbon composite. The concentration of methyl red was 100 mg/L, the composite's weight was 0.15 g and the pH was 4.4. The adsorption rate
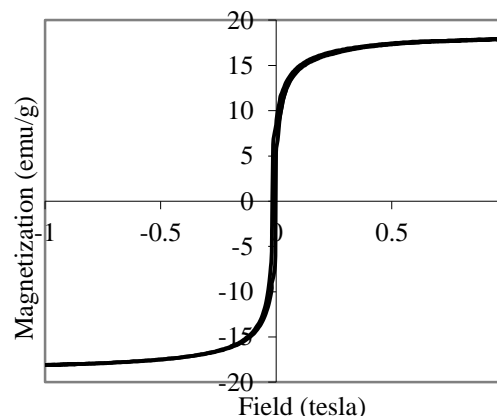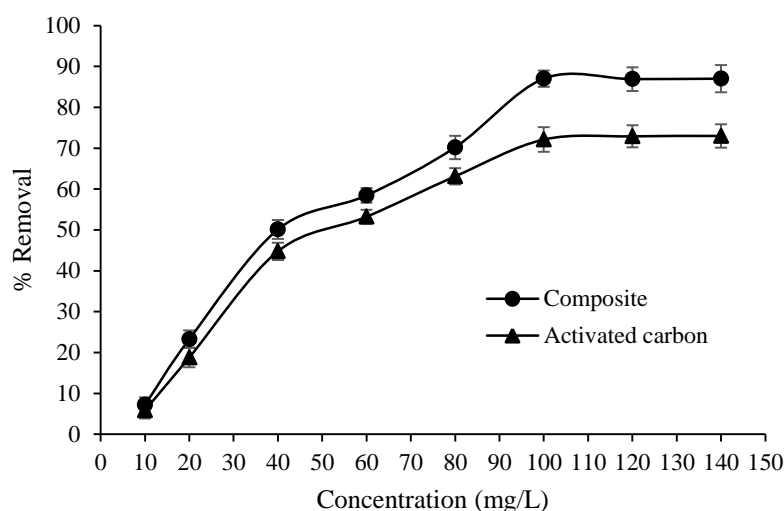

Figure 4. The Curve of magnetization of MnFe$_2$O$_4$-activated carbon composite
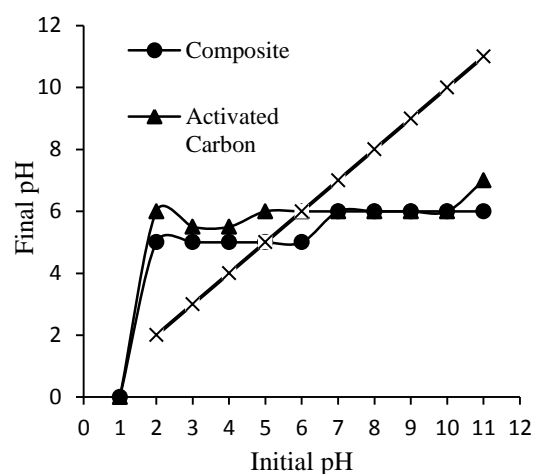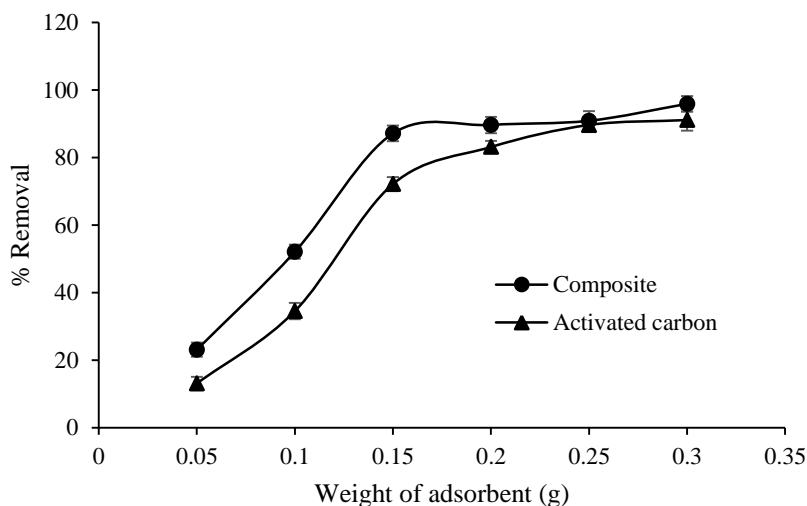

Figure 5. pH pzc of activated carbon and MnFe$_2$O$_4$-activated carbon composite

increased with the increase of contact time. At the contact time of 10-60 minutes, the adsorption process fast. At the contact time of 60 minutes, more than 50% of methyl red was adsorbed. After that, the adsorption process slowly and reached the optimum at the contact time of 100 minutes.

The amount of adsorbent is a parameter related to the cost of an effective amount of adsorbent to adsorb an adsorbate. **Figure 7** shows the effect of the weight of adsorbent that is the weight of 0.05-0.3 g, the concentration of methyl red dye of 100 mg/L, the contact time of 100 minutes and the pH of the solution of 4.4. The adsorption rate increases with the addition of adsorbent from 0.05 - 0.15 g. The increase in the amount of adsorbent also increases the number of active sites that can bind to the dye. However, with the addition of more adsorbent (> 0.15 g), the % of removal is relatively constant.

Figure 6. The effect of contact time on the adsorption of methyl red using activated carbon and MnFe$_2$O$_4$-activated carbon composite

Figure 7. The effect of adsorbent weight on the adsorption of methyl red using activated carbon and MnFe$_2$O$_4$-activated carbon composite

Heyeeye, Sattar, Chimpa, & Sirichote (2017) reported that an increase in the amount of adsorbent could decrease the adsorption capacity since the increase in the amount of adsorbent is not proportional to the increase in the amount of the dye adsorbed. Similarly, the study of Khan et al. (2018) showed the same pattern on methyl red adsorption using activated carbon.

Adsorption Isotherm

The adsorption capacity of activated carbon and MnFe$_2$O$_4$-activated carbon composite in removal methyl red can be illustrated using an adsorption isotherm model. Langmuir's isotherm theory is based on the assumption that the surface of the adsorbent is homogeneous, whereas Freundlich's isotherm illustrates that the adsorbent has a heterogeneous surface so that the adsorption process has an energy difference. The equation of Langmuir's and Freundlich's isotherm is expressed in the following equation:

$$\frac{C_e}{q_e} = \frac{1}{q_m \, b} + \frac{C_e}{q_m} \tag{1}$$

$$\log q_e = \log k_f + \frac{1}{n} \log C_e \tag{2}$$

in which q_m and b represent the adsorption capacity (mg/g) and the adsorption equilibrium (mg/L), whiles k_f and n are the Freundlich's constants expressing the adsorption capacity (mg/L) and the adsorption intensity (Hayeeye et al., 2017).

The Langmuir's and Freundlich's isotherm graphs are shown in **Figure 8** and **9**. The correlation coefficient (R^2) and other constants listed in **Table 3** indicate that the Langmuir's isotherm is more suitable for describing the methyl red dye adsorption process with both activated carbon and activated carbon-MnFe$_2$O$_4$ composite.

The favorable adsorption can be expressed with the dimensionless factor constant (R_L). The adsorption process is unfavourable if $R_L > 1$, favorable ($0 < R_L < 1$) and irreversible ($R_L = 0$). The value of R_L is calculated with the following equation:

$$R_L = \frac{1}{1+bC_0} \qquad (3)$$

Co is the initial concentration (mg/L). The data calculation reveals that the value of R_L of the activated carbon is 0.188 while of the composite is 0.244. This indicates that Langmuir isotherm is favorable.

The adsorption capacity of the composite is greater than activated carbon, although the active carbon surface area is larger than the composite. Nanomagnetic MnFe$_2$O$_4$ plays a role in the adsorption process. Several studies have reported that nanomagnetic MnFe$_2$O$_4$ can adsorb adsorbate. The studies by Zhong et al. (2015) reported that MnFe$_2$O$_4$ can adsorb congo red with an adsorption capacity of 118.76 mg/g. Ren et al. (2012) reported that nanomagnetic MnFe$_2$O$_4$ has an adsorption capacity against Pb (II) and Cu (II) of 333.3 and 952.4 µmol/g, respectively. Sezgin et al. (2016) removal of total chromium with adsorption capacity of 89.18 mg/g. The adsorption capacity in this study is greater than the adsorption of methyl red using silica coated Fe$_3$O$_4$ obtained of 49.50 mg/g (Rad, Irandoust, Amri, Feyzi, & Ja'fari, 2014).
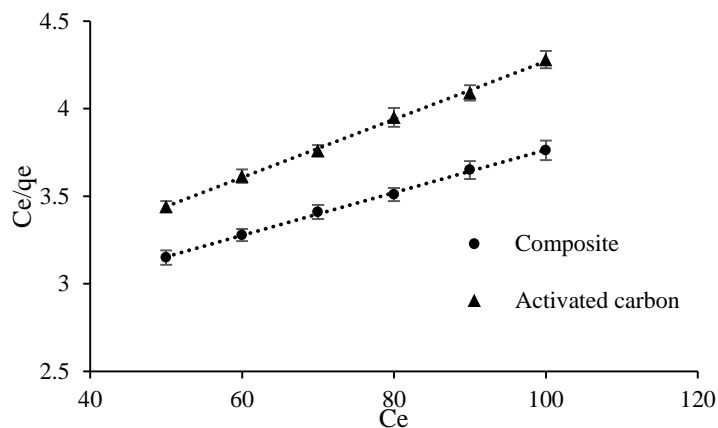
Figure 8. Langmuir isotherm of methyl red using activated carbon and MnFe$_2$O$_4$-activated carbon composite
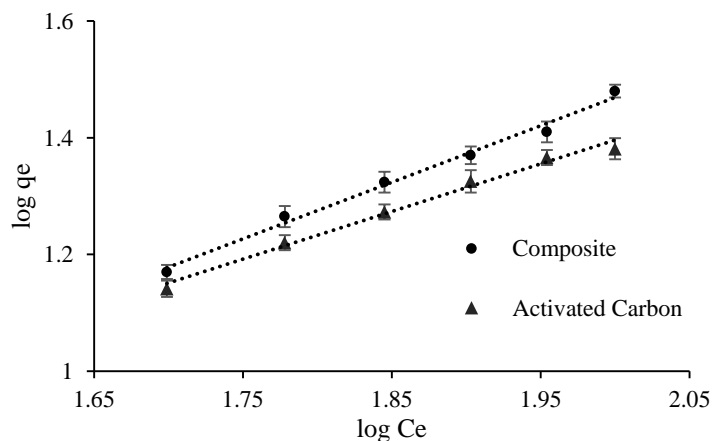
Figure 9. Freundlich isotherm of methyl red using activated carbon and MnFe$_2$O$_4$-activated carbon composite

Table 3. Parameters in the Langmuir and Freundlich models for methyl red adsorption

Adsorbent	Langmuir isotherm			Freundlich Isotherm		
	q_m	b	R^2	k_f	n	R^2
Activated carbon	60.24	0.043	0.9987	1.725	1.225	0.9889
Composite	81.97	0.031	0.9988	2.975	1.029	0.9897

Table 4. Kinetic parameters for adsorption methyl red by activated carbon and $MnFe_2O_4$-activated carbon composite

Kinetic parameters	Activated carbon	$MnFe_2O_4$-activated carbon composite
Pseudo-first-order		
R^2	0.905	0.9798
k_1 (1/min)	0.0011	0.0068
Pseudo-second-order		
R^2	0.9714	0.9916
k_2 (g/mg.min)	0.0131	0.0138

Kinetic Adsorption

Kinetic parameters and correlation coefficients of the adsorption process are shown in **Table 4**. From the table, it can be seen that the correlation coefficient value of the pseudo-second-order is greater than the pseudo-first-order for activated carbon and $MnFe_2O_4$-activated carbon composite. The equation of pseudo-first-order and pseudo-second-order is shown in the following equation:

$$\log (q_e - q_t) = \frac{\log q_e - k_1 t}{2.303} \tag{4}$$

$$\frac{t}{q_t} = \frac{1}{k_2 q_e^2} + \frac{1}{q_e t} \tag{5}$$

q_e and q_t are the number of adsorbates which are absorbed per unit of mass at equilibrium and every time, k_1 and k_2 are equilibrium constants for pseudo-first-order and pseudo-second- order. From the table, it can be seen that the correlation coefficient value of the pseudo-second-order is greater than the pseudo-first-order for activated carbon and $MnFe_2O_4$-activated carbon composite. The methyl red adsorption process is more compatible with pseudo-second-order. The adsorption mechanism depends on the interaction of the adsorbate and the adsorbent (Sarma, SenGupta, & Bhattacharyya, 2018).

CONCLUSIONS

In this study, the synthesis of $MnFe_2O_4$-activated carbon composite has been successfully performed by the co-precipitation method and it was applied to the removal of methyl red dye. The composite has magnetic properties with a saturation magnetization of 17.91 emu/g. The Langmuir isotherm is more suitable for describing methyl red dye adsorption in $MnFe_2O_4$-activated carbon composite. The adsorption capacity of $MnFe_2O_4$-activated carbon composite is greater than that of the activated carbon, namely 81.97 and 60.24 mg/g, respectively. Thus, $MnFe_2O_4$-activated carbon composite is potentially used as a commercial adsorbent for waste treatment.

REFERENCES

Aslibeiki, B., Kameli, P., Ehsan, E. H., Salamati, H., Muscas, G., Agostinelli, E., Foglietti, V., Casciardi, S., & Peddis, D. (2016). Solvothermal Synthesis of $MnFe_2O_4$ nanoparticles: The role of polymer coating on morphology and magnetic properties. *Journal of Magnetism and Magnetic Materials*, *399*, 236-244.

Audi, D.M. (2017). Synthesis of $MnFe_2O_4$ by co-precipitation method, its characterization, and photocatalytic study. *Research Journal of Chemical Science*, *7*(5), 7-10.

Deraz, N. M., & Alarifi, A. (2012). Controlled synthesis, physicochemical and magnetic properties of nano-crystalline Mn Ferrite System. *International*

Journal of Electrochemical Science, 7, 5534-5543.

Djilani C., Zaghdoudi, R., Bouchekima, B., Lallam, A., Modarressi, A., & Rogalski, M. (2015). Adsorption of dyes on activated carbon prepared from apricot stones and commercial activated carbon. *Journal of The Taiwan Institute of Chemical Engineering, 53*, 112-121.

Do, M.H., Phan, N.H., Nguyen, T.D., Pham, T.T.S., Nguyen, V.K., Vu, T.T.T., & Nguyen, T.K.P. (2011). Activated carbon/Fe_3O_4 nanoparticles composite: fabrication, methyl orange removal and regeneration by hydrogen peroxide. *Chemosphere*, *85*, 1269-1276.

Hayeeye, F., Sattar, M., Chinpa, W., & Sirichote, O. (2017). Kinetics and thermodynamics of Rhodamine B adsorption by gelatin/activated carbon composite beads. *Colloid and Surfaces A: Physicochemical and Engineering Aspect*, *513*, 259-266.

Hidarian, M., & Hashemian, S. (2014). Synthesize and characterization of sawdust/$MnFe_2O_4$ nanocomposite for removal of indigo carmine from aqueous solutions. *Oriental Journal of Chemistry*, *30* (4), 1753-1762.

Hou, X., Feng, J., Xu, X., and Zhang, M. (2010). Synthesis and characterizations of spinel $MnFe_2O_4$ by seed-hydrothermal route. *Journal of Alloys and Compounds*, *491*, 258-263.

Kanagesan, S., Aziz, S. B. A., Hashim, M., Ismail, I., Tamiselvan, S., Alitheen, N. B. B. M., Swany, M. K., & Rao, B. P. C. (2016). Synthesis, characterization and in vitro evaluation of manganese ferrite ($MnFe_2O_4$) nanoparticles for their biocompatibility with murine breast cancer cell (4T1). *Molecules, 21*(3), 312-320.

Khan, E. A., Shahjahan, & Khan, T. A. (2018). Adsorption of methyl red on activated carbon derived from custard apple (*Annona squamosa*) fruit shell: equilibrium isotherm and kinetic studies. *Journal of Molecular Liquids*, *249*, 1195-1211.

Li, J., Yuan, H., Li, G., Liu, Y., & Leng, J. (2010). Cation distribution dependence of magnetic properties of sol-gel prepared $MnFe_2O_4$ spinel ferrite

nanoparticles. *Journal of Magnetism and Magnetic Materials*, *322*, 3396-3400.

Osmokrovic, P., Jovalekic, C., Manojlovic, D., & Pavlovic, M. B. (2006). Synthesis of $MnFe_2O_4$ nanoparticles by mechanochemical reaction. *Journal of Optoelectronics and Advanced Materials*, *8*(1), 312-314.

Rad, M. S., Irandoust, M., Amri, S., Feyzi, M., & Ja'fari, F. (2014). Removal, preconcentration, and determination of methyl red in water samples using silica-coated magnetic nanoparticles. *Journal of Applied Research in Water and Wastewater*, *1*, 6-12.

Ren, Y., Li, N., Feng, J., Luan, T., Wen, Q., Li, Z., & Zhang, M. (2012). Adsorption of Pb(II) and Cu (II) from aqueous solution on magnetic porous ferrospinel $MnFe_2O_4$. *Journal of Colloid and Interface Science*, *367*, 415-421.

Riyanti, F., Hariani, P.L., Purwaningrum, W. (2018). Adsorption of Rhodamine B from aqueous solution by $MnFe_2O_4$ nanomagnetic. *Pollution Research*, *37*(1), 97-104.

Sam, S., & Nesaraj, A. S. (2011). Preparation of nanoceramics particles by soft chemical route. *International Journal of Applied Science and Engineering*, *9*(4), 223-239.

Santhi, T, Manonmani, S., & Smitha, T. (2010). Removal of methyl red from aqueous solution by activated carbon prepared from the *Annona squmosa* seed by adsorption. *Chemical Engineering Research Bulletin*, *14*, 11-18.

Sarma, G. K., SenGupta, S., & Bhattacharyya, K. G. (2018). Adsorption of monoazo dyes (Crocein orange G and Procion Red MX5b) from water using raw and acid treated montmorillonite K10: insight into kinetics, isotherm, and thermodynamic parameters. Water Air Soil Pollution, *10*, 229-312.

Saxena, R., & Sharma, S. (2016). Adsorption and kinetic studies on the removal of methyl red from aqueous solutions using low-cost adsorbent: guar gum powder. *International Journal of Scientific Engineering Research*, *7*(3), 675-683.

Sezgin, N., Yalcin, A., & Koseoglu, Y. (2016). $MnFe_2O_4$ nano spinels as potential sorbent for adsorption of chromium

from industrial wastewater. *Desalination and Water Treatment*, *57*(35), 16495-16506.

Shanmugavel, T., Raj, S. G., Kumar, G.R., & Rajarajan, G. (2014). Synthesis and structural analysis of nanocrystalline MnFe$_2$O$_4$. *Procedia*, *54*, 159-163.

Tan, I. A. W., Ahmad, A. L., & Hameed, B. H. (2008). Preparation of activated carbon from coconut husk: optimization study on removal of 2,4,6-trichlorophenol using response surface methodology. *Journal of Hazardous Materials*, *153*, 709-717.

Tawainella, R. D., Riana, Y., Fatyati, R., Amelliya, Kato, T., Iwata, S., & Suharyadi, E. (2014). Sintesis nanopartikel manganese ferrite (MnFe$_2$O$_4$) dengan metode kopresipitasi dan karakterisasi sifat kemagnetannya. *Jurnal Fisika Indonesia*, *XVIII* (52), 1-7.

Xia, S., X. Xu, C. Xu., Wang, H., Zhang, X., & Liu, G. (2016). Preparation, characterization, and phosphate removal and recovery of magnetic MnFe$_2$O$_4$ nanoparticles as adsorbents. *Environmental Technology*, *37*(7), 795-804.

Yamaguchi, N.U., Bergamasco, R., & Hamoudi, S. (2016). Magnetic MnFe$_2$O$_4$-graphene hybrid composite for efficient removal of glyphosate from water. *Chemical Engineering Journal*, *295*, 391-402.

Zhong, X., Yang, J., Chen, Y., Qiu, X., & Zhang, Y. (2015). Synthesis of magnetically separable MnFe$_2$O$_4$ nanocrystals via salt-assisted solution combustion method and their utilization as dye adsorbent. *Journal of the Ceramic Society of Japan*, *123*, 394-398.